

Taku M. Saitoh · Shin Nagai · Jun Yoshino
Hiroaki Kondo · Ichiro Tamagawa · Hiroyuki Muraoka

Effects of canopy phenology on deciduous overstory and evergreen understory carbon budgets in a cool-temperate forest ecosystem under ongoing climate change

Received: 27 June 2014 / Accepted: 10 December 2014 / Published online: 23 December 2014
© The Ecological Society of Japan 2014

Abstract Canopy phenology is a key regulator of carbon cycling in forest ecosystems. To clarify its possible effects on carbon budgets of forest ecosystems under ongoing climate change, we developed a canopy-phenology model for a forest with deciduous overstory and evergreen understory based on in situ observations, and used it to improve an ecosystem carbon budget model. Under future conditions (2068–2073) based on the IPCC SRES A1B scenario, leaf expansion began 12.5 ± 1.9 days earlier and leaf-fall ended 11.3 ± 2.7 days later than under current conditions (2002–2007). We also estimated the possible influence of altered light availability on understory vegetation. Even though the photosynthetically active period in the understory (i.e., from the end of spring snowmelt to the beginning of late-autumn snow cover) expanded by 15.7 ± 15.7 days, the total downward photosynthetic photon flux density above this vegetation during the snow-free period decreased by 11.8 % because of changing overstory canopy phenology. The net effect of these changes increased ecosystem-level annual gross primary production (GPP) by 12.5 %, net primary production (NPP) by 12.0 %, and net eco-

system production by 12.1 %, especially in late spring (when the highest solar radiation occurred). The increased GPP and NPP were mostly attributable to changes in overstory vegetation. Our analysis indicates that understanding the temporal variation of canopy phenology dynamics and snow cover is important and that the effects of vegetation phenology on the carbon cycle should be evaluated in future climate change studies.

Keywords Canopy phenology · Carbon budget · Climate change · Snow cover · Understory vegetation

Introduction

Long-term trends and interannual variability in the canopy phenology of forests, such as changes in the timing of leaf expansion and leaf-fall, are major concerns in studies of current and future carbon cycles in forest ecosystems, since these changes directly affect photosynthetic CO₂ uptake and respiratory CO₂ release in those ecosystems (Baldocchi 2008). Recent studies of temperate vegetation have revealed that spring phenology of events such as leaf unfolding and expansion has gradually moved earlier in response to climate change in the Northern Hemisphere (by 1.2–1.6 days per decade; Schwartz et al. 2006; Piao et al. 2007) and, regionally, in Europe (2.0–2.8 days per decade; Menzel and Fabian 1999; Menzel et al. 2006; Piao et al. 2007), Asia (0.8–4.0 days per decade; Matsumoto et al. 2003; Chen and Xu 2012), and North America (1.8 days per decade; Richardson et al. 2006). In addition, autumn canopy phenology for events such as leaf color development and leaf-fall has been delayed under climate change in the Northern Hemisphere (by 1.4 days per decade; Piao et al. 2007), Europe (1.6 days per decade; Menzel and Fabian 1999), Asia (1.6–2.2 days per decade; Matsumoto et al. 2003; Chen and Xu 2012), and North America (2.8 days per decade; Piao et al. 2007). Piao et al. (2007)

T. M. Saitoh (✉) · I. Tamagawa · H. Muraoka
River Basin Research Center, Gifu University, 1-1 Yanagido,
Gifu 501-1193, Japan
E-mail: taku@green.gifu-u.ac.jp
Tel.: +81-58-293-3388
Fax: +81-58-293-2062

S. Nagai
Department of Environmental Geochemical Cycle Research, Japan
Agency for Marine-Earth Science and Technology, 3173-25 Showa-
machi Kanazawa-Ku, Yokohama 236-0001, Japan

J. Yoshino
Graduate School of Engineering, Gifu University, 1-1 Yanagido,
Gifu 501-1193, Japan

H. Kondo
National Institute of Advanced Industrial Science and Technology
(AIST), AIST Tsukuba West, 16-1 Onogawa, Tsukuba, Ibaraki
305-8569, Japan

reported that such long-term phenological shifts have increased annual gross primary production (GPP) and net primary production (NPP), and stated that a change in phenology in response to rising global temperatures was one of the most important factors that would affect future vegetation productivity in northern terrestrial ecosystems. Similarly, recent field studies have suggested that interannual variation in the timing of spring and autumn phenology transitions controlled variations of net ecosystem production (NEP) in forest ecosystems (Churkina et al. 2005; Richardson et al. 2009; Wu et al. 2013a, b).

Ecosystem models have been developed to explain the carbon cycles of forest ecosystems and to elucidate their responses to changes in meteorological factors and canopy phenology (Richardson et al. 2013). Despite great efforts to quantify environmental responses and to construct models of canopy phenology, current ecosystem models cannot always accurately represent key phenological events such as the start of leaf expansion and end of leaf-fall (Richardson et al. 2012). One of the main reasons is that expected changes in canopy phenology under climate change will differ among regions (Botta et al. 2000; Schwartz et al. 2006; Piao et al. 2007). Indeed, the sensitivity of canopy phenology to environmental change varies among biomes (Morin et al. 2009). For instance, Nagai et al. (2014) suggested that the start of leaf expansion and end of leaf-fall was more sensitive to temperature in deciduous broadleaf forests than in deciduous coniferous forests. Thus, further research is required to improve current ecosystem models by taking advantage of phenological observations from as wide a range of environmental and climatic conditions as possible, and to evaluate the impact of changing canopy phenology on carbon budgets under ongoing climate change in a range of forest types and regions (Jeong et al. 2012; Chung et al. 2013; Richardson et al. 2013).

In cool-temperate deciduous forests of eastern Asia, evergreen dwarf bamboo is widespread in the understory (Ito and Hino 2004; Sakai et al. 2006; Tang et al. 2007; Takagi et al. 2009; Yashiro et al. 2012). Therefore, the contribution of this vegetation to forest ecosystems is another fundamental issue in determining their carbon budgets under current and future environments. Earlier leaf expansion and later leaf-fall of overstory vegetation under ongoing climate change will affect micrometeorological conditions in and below the overstory, thereby affecting carbon, water, and heat budgets of the understory vegetation. Furthermore, in a cool-temperate region, timing of the end of snowmelt in spring and of the start of snow cover in early winter may determine the photosynthetically active period of understory evergreen vegetation, thereby affecting its carbon, water, and heat budgets. Thus, researchers should seek ways to predict changes in snow cover and overstory canopy phenology to determine their effects on understory vegetation and evaluate possible changes in the functional roles of overstory and understory vegetation and their effects on total ecosystem carbon budgets under the climate change. In Japan, deciduous broadleaf forest with evergreen

understory vegetation is a common vegetation type, and thus represents an important ecosystem for such studies.

The purposes of the present study were to predict changing timing of the start of leaf expansion and end of leaf-fall under ongoing climate change, to clarify possible effects of forest canopy phenology on the overstory and understory carbon budgets of a forest ecosystem under that climate change, and to derive implications of canopy phenological observations for carbon budget estimates. To do so, we developed a canopy-phenology model based on in situ observations and an improved ecosystem model that incorporates our phenology model, and used the improved model to investigate response of the deciduous overstory and evergreen understory carbon budgets to changing environmental factors and canopy phenology.

Methods

Site description

Our study was conducted at the Takayama deciduous broadleaf forest site (36°08'46"N, 137°25'23"E, 1420 m a.s.l.), which belongs to the AsiaFlux network (AsiaFlux site code TKY; <http://www.asiaflux.net>) and the Japan Long-Term Ecological Research network (JaLTER, <http://www.jalter.org>). The site is near Takayama City in the central part of Japan's main island. This region has a cool-temperate climate that is influenced by the Asian monsoon, and is characterized by mild, humid springs and autumns, hot, humid summers, and cold, snowy winters. Table 1 summarizes vegetation and climate characteristics of TKY. The leaf area index (LAI) in the overstory deciduous broadleaf forest has a clear seasonal pattern, but LAI in the dense evergreen dwarf bamboo understory remains almost constant throughout the year (Nasahara et al. 2008). Saigusa et al. (2002) and Ohtsuka et al. (2005) provide more detailed descriptions of TKY. The micrometeorological and tower-based flux measurement dataset from 2001 to 2007 at TKY was obtained from the AsiaFlux database.

Ecosystem model

We used version 1.0 of the National Center for Atmospheric Research Land Surface Model (NCAR LSM; Bonan 1996), which simulates carbon, water, and heat cycles over the land surface. We adapted the model to account for canopy phenology and the understory carbon budget. Here, we briefly describe the improved canopy phenology and carbon budget calculations.

Canopy phenology submodel

As noted in the Introduction, the sensitivity of canopy phenology to environmental changes varies by forest

Table 1 Summary of vegetation and climate characteristics at Takayama deciduous broadleaf forest site (TKY)

	Characteristics
Overstorey vegetation type	Deciduous broadleaf forest
Overstorey dominant species	<i>Betula ermanii</i> Cham., <i>Quercus crispula</i> Blume ^a
Height of tree canopy	13–20 m ^b
Tree age	Approx. 60 years ^c
Annual maximum overstorey leaf area index	Approx. 5 m ² m ^{-2d}
Understorey vegetation	Evergreen dwarf bamboo [(<i>Sasa senanensis</i> (Franch. et Sav.) Rehder) ^d
Understorey leaf area index	Approx. 1.7 m ² m ⁻² throughout the year ^d
Annual mean air temperature	6.5 °C ^e
Soil type	Cambisol (Brown forest soil affected by volcanic ash) ^f
Annual mean rainfall	2089 mm ^g
Snow-cover period	Early December through mid-April ^g

^aOhtsuka et al. (2005)^bSaitoh et al. (2012b)^cNagai et al. (2013)^dNasahara et al. (2008)^e1996–2009 average at TKY^fJia and Akiyama (2005)^g1996–2009 average at Takayama field station of Gifu University, ~500 m south of TKY

type and region. Therefore, it is crucial to construct an empirical phenology model for each biome and study region. In the original NCAR LSM, LAI can be input at monthly intervals and is represented by a single value at the midpoint of each month (e.g., 15 January, 14 February). The interpolated LAI is used to calculate hourly carbon, water, and heat cycles during that month. We developed a canopy phenology submodel based on observed relationships between canopy phenology and effective cumulative temperature to account for seasonal changes of canopy LAI as a function of air temperature, with changes determined at daily time step (Fig. 1). Nagai et al. (2013) detected dates of the start of leaf expansion and of the end of leaf-fall in the overstorey canopy using daily canopy-surface images at TKY from 2004 to 2011. They examined those dates and their relationships with cumulative effective temperature. They found that leaf expansion began when the cumulative effective temperature from the first day of the year (based on a 2 °C threshold) exceeded 255.4 ± 18.8 °C (average \pm standard deviation) in the spring, and that leaf-fall ended when that temperature after 1 August (based on an 18 °C threshold) fell to less than -375.1 ± 32.8 °C in autumn. We adopted these two thresholds for the start of leaf expansion and end of leaf-fall for our phenology submodel (Fig. 1).

Carbon budget scheme

In the original NCAR LSM, the carbon budget was separated into CO₂ uptake by photosynthesis (i.e., GPP) and respiratory CO₂ release by plants and decomposition (i.e., R_{au} for autotrophic respiration and R_h for heterotrophic respiration). Overstorey photosynthesis is coupled to stomatal resistance via parameterization based on the models of Farquhar et al. (1980) and Collatz et al. (1991) for C₃ plants. See “Appendix” for a detailed description of the calculation schemes for

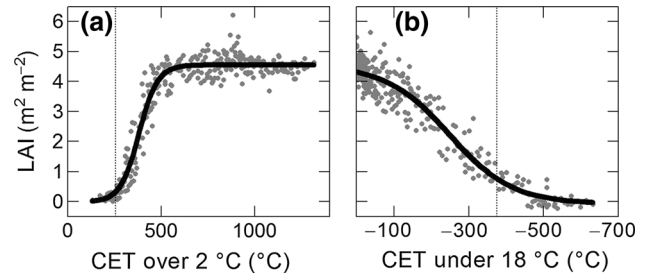


Fig. 1 Leaf area index (LAI) of forest canopy as function of cumulative effective temperature (CET) during (a) leaf-expansion and mature periods, and (b) leaf-fall period. LAI was estimated by measuring incident photosynthetic photon flux density above the deciduous forest canopy and above the understory evergreen dwarf bamboo canopy from 2004 to 2009, based on the Monsi-Saeki theory (see Saitoh et al. 2012a for detailed description). Solid line represents interpolated LAI calculated using a sigmoid model. Vertical dotted lines indicate critical temperatures for (a) start of leaf expansion and (b) end of leaf-fall, based on camera image analysis of forest canopy by Nagai et al. (2013)

overstorey photosynthesis. Because the original model treats the vegetation canopy as a monolayer, we added an understory layer to account for photosynthesis and respiration of evergreen dwarf bamboo. Then, gross leaf photosynthesis (A_u) of the understory of that bamboo was calculated using the equation proposed by Thornley (1976):

$$A_u = \frac{\alpha I + A_{\max} - \sqrt{(\alpha I + A_{\max})^2 - 4\theta\alpha I A_{\max}}}{2\theta}, \quad (1)$$

where α is the apparent quantum yield of photosynthesis ($\mu\text{mol CO}_2 \text{ mol}^{-1} \text{ photons}$), I is photosynthetic photon flux density (PPFD) absorbed by the leaf (which is assumed to be 85 % of incident PPFD at the height of understory leaves), A_{\max} is the light-saturated photosynthetic rate, and θ is a factor that describes convexity of the light-response curve (Muraoka et al. 2010). Fi-

nally, we multiplied the single-leaf photosynthetic rate calculated using this equation by 1.7, which is the LAI of evergreen dwarf bamboo and which does not change much during the year (Nasahara et al. 2008). The photosynthetically active period of the understory was determined from the presence of snow cover, which was estimated by a simple mass-balance function determined using gains from the flux of snow at the ground surface and surface dew, and losses from snowmelt and sublimation (Bonan 1996).

In the improved model, the respiration component is partitioned into R_h , overstory R_{au} , and understory R_{au} . R_h is determined as a function of volumetric soil water content at depth 1 m and temperature of the surface soil layer. Parameters include half the field capacity, half the saturated capacity, soil carbon content to depth 1 m (kg m^{-2}), respiration rate ($\mu\text{mol CO}_2 \text{ kg}^{-1} \text{ s}^{-1}$) at 10°C , and a temperature sensitivity parameter. Overstory R_{au} and modified understory R_{au} both consist of maintenance respiration and growth respiration. See “Appendix” for a detailed description of the calculation schemes for overstory R_{au} . Maintenance respiration of the understory vegetation (R_{um}) is the sum of aboveground (R_{uma}) and root (R_{umr}) respiration:

$$\begin{aligned} R_{um} &= R_{uma} + R_{umr} \\ &= [V_{uba} \cdot R_{ua25} + V_{ubr} \cdot R_{ur25}] a_{rm} \frac{T_g - 25}{10}, \end{aligned} \quad (2)$$

where V_{uba} is the aboveground biomass of understory vegetation (0.64 kg m^{-2} ; Yashiro et al. 2012), R_{ua25} is the aboveground respiration of that vegetation at 25°C ($\mu\text{mol CO}_2 \text{ kg}^{-1} \text{ s}^{-1}$), V_{ubr} is root biomass of that vegetation (0.54 kg m^{-2} ; Yashiro et al. 2012), R_{ur25} is root respiration of that vegetation at 25°C ($\mu\text{mol CO}_2 \text{ kg}^{-1} \text{ s}^{-1}$), a_{rm} is a temperature-sensitivity parameter, and T_g is ground surface temperature. We used fixed values of V_{uba} and V_{ubr} for both present and future simulations. Growth respiration by the understory vegetation (R_{ug}) is proportional to understory NPP (NPP_u):

$$R_{ug} = a_{ugr} \cdot \text{NPP}_u, \quad (3)$$

where a_{ugr} is a proportionality coefficient.

Future climate scenarios

We chose the Intergovernmental Panel on Climate Change (IPCC) Special Report on Emissions Scenarios (SRES) A1B emission scenario provided by the Climate Change Information Database of the Disaster Prevention Research Institute, Kyoto University (<http://mhri.dpri.kyoto-u.ac.jp/database/index.html?LANG=EN>), which was defined in a format compatible with the CMIP3 multi-model dataset. The projected increase of global temperature in SRES A1B lies between those in the RCP6.0 and RCP8.5 scenarios in the more recent CMIP5 multi-model dataset from the 2040s to 2060s (IPCC 2013). To reduce uncertainty, we used the

ensemble average of four models (CGCM3.1(T47), CSIRO-Mk3.0, MIROC3.2(medres), and UKMO-HadCM3) with relatively strong reproducibility for the current climate in Japan (Michihiro et al. 2011). The database provided the difference between (or ratio of) monthly meteorological average values for current (1980–1999) and projected future (2046–2065) conditions. Therefore, instead of using actual climate model outputs, we used the difference in air temperature and the precipitation ratio between current and future projections, and adjusted measured hourly meteorological values from 2001 to 2007 at TKY by adding the difference for air temperature and multiplying by the ratio for precipitation. Here, we assumed that the difference and ratio values between the 2001–2007 and 2067–2073 periods were the same as those between 1980–1999 and 2046–2065. Note that (1) maximum and minimum temperature increases were 2.2°C during the mature leaf period (June–September) and 2.0°C during the leaf-fall period (October–November) and (2) maximum and minimum precipitation increase ratios were 1.13 during the mature period and 1.00 during the leaf-fall period. To eliminate the effect of elevated CO_2 from our results, we conducted our simulations based on the assumption of a stable atmospheric CO_2 concentration for the period 2001–2073.

Model simulations

Original model simulation under current climate

The original NCAR LSM is driven at an hourly time step by values of shortwave and longwave radiation, air temperature, wind speed, precipitation, and relative humidity. We ran the model with an hourly measurement dataset from 2001 to 2007. To improve the original model’s performance for a given forest, we adjusted and tuned the default parameter values using data from our study site. Saitoh et al. (2012b) provides detailed information on the simulation using the original model. In the original NCAR LSM, LAI can be input at monthly intervals, and the interpolated LAI is used in simulation. In the present study, we used the 6-year average seasonal pattern of LAI, which was estimated by measuring incident photosynthetic photon flux density above the deciduous forest canopy and above the understory evergreen dwarf bamboo canopy from 2004 to 2009, based on the Monsi-Saeki theory (Saitoh et al. 2012a). This means that we did not consider temperature sensitivity of canopy phenology in the original model simulation. We initialized the model on 1 January 2001 using observed values and then simulated the ecosystem from 1 January 2001 through 31 December 2007. To eliminate the effect of the initialization on carbon budget estimates, we used simulated results from 1 January 2002 through 31 December 2007 and then compared them with those obtained from the improved model (described in the next section).

Improved model simulation under current and future climates

The improved NCAR LSM is driven at an hourly time step using the same meteorological values as the original model. We ran the model with the hourly measurement dataset from 2001 to 2007 and predicted future hourly meteorological dataset from 2067 to 2073. As with the simulation using the original model, we adjusted and tuned the default parameter values using data from our study site. First, we improved model parameters of tree height, canopy bottom, stem biomass, root biomass, displacement height, and roughness length using measured values at TKY (Saitoh et al. 2012b). We further tuned the model based on eddy-covariance data (seasonal patterns and annual values of GPP, ecosystem respiration [RE], and NEP) and biometric data (annual values of NPP, NEP, and R_h) from January through December 2001 at TKY. We used the measured and adjusted parameters in the simulations. We initialized the model on 1 January 2001 using observed values and then simulated the ecosystem from 1 January 2001 through 31 December 2007. Similarly, we initialized the model on 1 January 2067 and then simulated the ecosystem from 1 January 2067 through 31 December 2073. To eliminate the effect of the initialization on carbon budget estimates, we used simulated results from 1 January 2002 through 31 December 2007 to represent the current climate and those from 1 January 2068 through 31 December 2073 to represent the future projection. That is, we discarded results from the first year, which served as the model spinup period.

Results

Model performance

Annual carbon fluxes estimated by the original and improved models were similar to those estimated by means of tower flux and biometric measurements (Table 2). Daily carbon fluxes simulated using the improved model were generally more strongly correlated with measured fluxes for GPP, RE, and NEP during leaf-expansion, mature, leaf-fall, and annual periods, relative to the original model (Table 3). The improved model successfully reproduced measured carbon fluxes of GPP, RE, and NEP in terms of seasonal variations during the leaf-expansion and leaf-fall periods, when the effects of understory vegetation dominated, and during the mature period, when the effects of overstory vegetation dominated (Fig. 2). The magnitude and interannual variations of annual carbon fluxes in the improved model simulation agreed with measured ones, except for the 2004 data, when strong tropical cyclones (typhoons) struck Japan. Slopes of the regressions for the simulated values as a function of measured ones were 0.91 for GPP ($R^2 = 0.36$, $P = 0.29$), 0.61 for RE ($R^2 = 0.64$, $P = 0.10$), and 1.10 for NEP ($R^2 = 0.45$, $P = 0.22$) for

Table 2 Performance of original and improved models of annual cumulative carbon fluxes at Takayama deciduous broadleaf forest site (TKY)

		Carbon flux (Mg C ha ⁻¹ year ⁻¹)		
		Original model	Improved model	Measurement
Production				
GPP	11.2		10.1	10.0 ^a
NPP	6.1		5.4	6.5 ^b
NPP-	–		4.9	5.4 ^b , 3.2 ^c
^o NPP-	–		0.5	1.1 ^b
^u NEP	2.8		2.1	2.5 ^a , 2.1 ^b
Respiration				
RE	8.4		8.0	7.5 ^a
R_{soil}	6.2		6.6	7.1 ^b
R_h	3.3		3.3	3.9 ^b
R_{root}	2.9		3.3	3.2 ^b

Validation includes some uncertainty arising from difference in periods used for models and measurement data per footnotes (b) and (c)

GPP gross primary production, NPP net primary production, NPP_o overstory NPP, NPP_u understory NPP, NEP net ecosystem production, RE ecosystem respiration, R_{soil} soil respiration, R_h heterotrophic respiration, R_{root} root respiration

^a6-year average (2002–2007) estimated using eddy-covariance method (Ohtsuka et al. 2009; AsiaFlux database)

^b5-year average (1999–2003) estimated using biometric measurements (Ohtsuka et al. 2007)

^c8-year average (1999–2006) estimated using biometric measurements (Ohtsuka et al. 2009)

the 5-year dataset excluding 2004. Consequently, our phenology model simulated carbon budgets at TKY reasonably well, except in a year with extreme events (in this case, a series of typhoons), and can therefore be used to evaluate the impact of canopy phenology on carbon budgets.

Changes in overstory and understory phenology

Figure 3 shows the projected changes in overstory and understory phenology under global warming. Under the future conditions, overstory leaf expansion began 12.5 ± 1.9 days earlier and leaf-fall ended 11.3 ± 2.7 days later (Fig. 3a). As a result, the predicted growing period increased by 23.8 ± 2.6 days. Temperature sensitivities at the start of leaf expansion, end of leaf-fall, and for the growing period as a whole were 6.2, 5.8, and 12.0 days °C⁻¹, respectively.

We also estimated the photosynthetically active period of the understory evergreen vegetation (i.e., from the end of snowmelt in spring to beginning of snow cover in late autumn) under current and future climate conditions. Under the future conditions, the spring snowmelt ended 13.2 ± 11.2 days earlier and snow cover in late autumn began 2.5 ± 4.7 days later, extending the photosynthetically active period by 15.7 ± 15.7 days. Temperature sensitivity of that period was 7.5 days °C⁻¹.

Table 3 Errors in daily gross primary production (GPP), ecosystem respiration (RE) and net ecosystem production (NEP), estimated using original and improved models, based on comparison with tower-flux measurements during leaf-expansion (April–May), mature (June–September), leaf-fall (October–November), and annual periods

Period	Carbon flux	Original model error (g C m ⁻² day ⁻¹)			Improved model error (g C m ⁻² day ⁻¹)		
		RMSE	MBE	R ²	RMSE	MBE	R ²
Leaf expansion	GPP	1.15	-0.19	0.47***	<i>1.00</i>	0.36	0.45***
	RE	0.36	0.07	0.70***	<i>0.39</i>	-0.05	0.69***
	NEP	1.09	-0.26	0.27***	<i>0.87</i>	0.42	0.31***
Mature	GPP	1.93	0.73	0.57***	<i>1.70</i>	-0.11	0.76***
	RE	0.56	0.28	0.81***	<i>0.54</i>	0.42	0.92***
	NEP	1.53	0.44	0.61***	1.67	-0.55	0.69***
Leaf-fall	GPP	1.70	0.93	0.52***	<i>0.92</i>	0.43	0.63***
	RE	0.49	0.37	0.81***	<i>0.27</i>	0.07	0.86***
	NEP	1.32	0.55	0.31***	0.78	0.34	0.47***
Annual	GPP	1.42	0.33	0.86***	<i>1.14</i>	0.03	0.89***
	RE	0.43	0.23	0.94***	<i>0.40</i>	0.13	0.96***
	NEP	1.16	0.09	0.76***	<i>1.08</i>	-0.10	0.79***

Italicized values indicate improvements (decreased error terms) by improved model
 RMSE root-mean-square error, MBE mean bias error, R² coefficient of determination
 *** indicates significance at $P < 0.001$

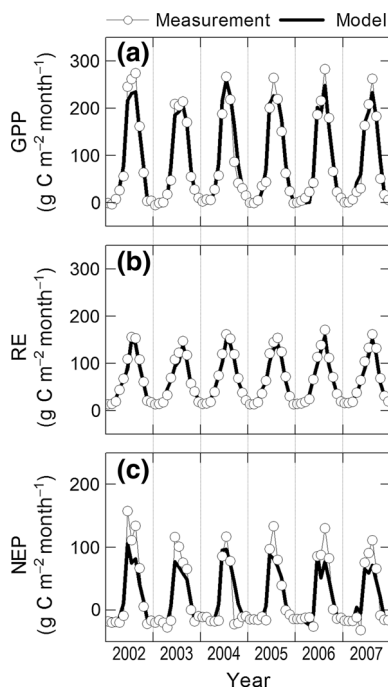


Fig. 2 Monthly variations of (a) gross primary production (GPP), b ecosystem respiration (RE), and c net ecosystem production (NEP) derived from tower-flux measurements and improved model

Changes in carbon budget

Annual whole-ecosystem GPP, NPP, NEP, RE, R_{au} , and R_{h} were greater under future conditions than current conditions, by 12.5, 12.0, 12.1, 12.6, 13.0, and 12.0 %, respectively (Fig. 4a). Temperature sensitivities of annual GPP, NPP, NEP, RE, R_{au} , and R_{h} were 60.1, 30.8, 12.2, 47.9, 29.3, and 18.6 g C m⁻² year⁻¹ °C⁻¹, respectively. Increased production and respiration were mostly attributable to changes in the overstory decidu-

ous vegetation (Fig. 4b). However, the understory vegetation showed decreased GPP and NPP, and no change in R_{au} (Fig. 4c). As a result, the contribution of understory GPP to the whole-ecosystem GPP decreased slightly, from 11.3 % under the current climate to 9.1 % under the projected future climate.

The whole-ecosystem and overstory GPP increased throughout the growing season under the future climate scenario (Fig. 5a, b), whereas that for the understory vegetation increased in April and decreased in May, with only minor changes in other months (Fig. 5c). There were no impacts of drought or heavy snowfall under the projected future climate (data not shown). Although the advance in date of leaf expansion was similar to the delay in the end of leaf-fall, the increased whole-ecosystem production during the leaf-expansion period accounted for the majority of the total annual increase, accounting for 46 % of the total increase in GPP, 63 % in NPP, and 135 % in NEP (Table 4).

RE values under the projected future climate increased in all months compared with those under the current climate (Fig. 6a), owing to increases in both R_{au} and R_{h} (Fig. 6b). R_{h} contributed 48 % of the overall RE increase during summer. The smallest contribution of R_{h} to the increased RE was in spring and autumn. In addition, the increase of R_{h} during May was smaller than those in April and June (Fig. 6b), because the earlier leaf expansion delayed the soil surface temperature increase that would have occurred during this period (data not shown).

Discussion

Our study leads to four main findings. (1) It revealed the influence of extreme weather conditions in the Asian monsoon region (specifically, the series of typhoons that struck Japan in 2004; Fig. 2). (2) It demonstrated the

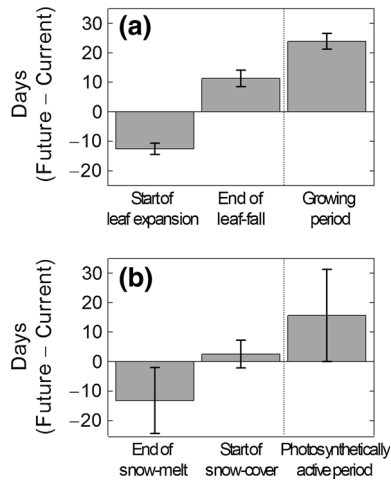


Fig. 3 Projected changes in **a** overstory and **b** understory phenology under global warming. Positive values represent later and negative ones earlier timing in the future projection (2068–2073) relative to the current climate (2002–2007). *Range bars* show standard deviation for data from the 6 years of each period

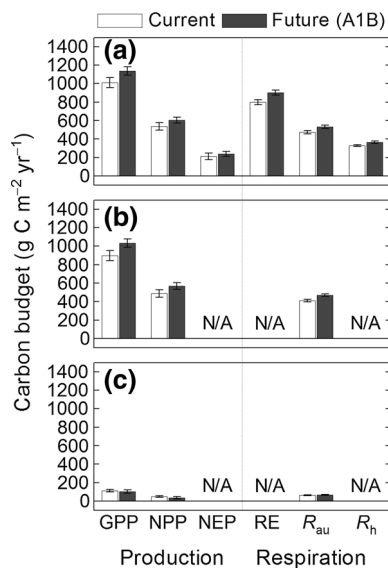


Fig. 4 Simulated annual total gross primary production (GPP), net primary production (NPP), net ecosystem production (NEP), ecosystem respiration (RE), autotrophic respiration (R_{au}), and heterotrophic respiration (R_h) under future (2068–2073) and current (2002–2007) climates for **(a)** whole ecosystem, **b** overstory vegetation, and **c** understory vegetation. *N/A* indicates not available. *Range bars* show standard deviation for data from the 6 years of each period

importance of quantifying canopy phenology based on long-term in situ observations (Table 3). (3) It clarified the consequences of different patterns of forest canopy and understory productivity that result from variations in light availability associated with phenological changes (Figs. 3, 4, 5; Table 4). (4) It illuminated the effects of seasonal variations and climate change on phenology (Figs. 5, 6). As a result, the improved model revealed the

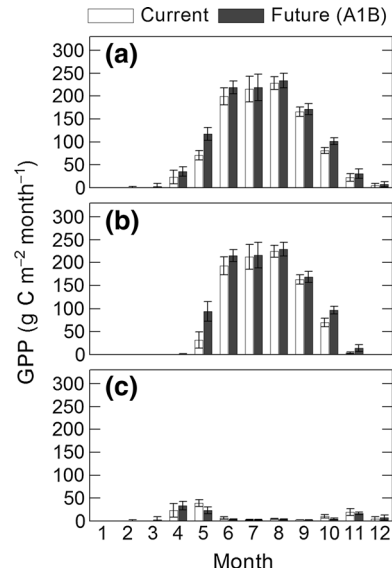


Fig. 5 Simulated seasonal variations of gross primary production (GPP) under current (2002–2007) and future (2068–2073) climates for **(a)** whole ecosystem, **b** overstory vegetation, and **c** understory vegetation. *Range bars* show standard deviation for data from the 6 years of each period

importance of incorporating vegetation phenology in carbon budget models.

A key limitation of the current study is the lack of ability to simulate unpredictable extreme events. Because both plant physiology and phenology respond to such events (e.g., tropical cyclones), canopy phenology models cannot account for them without including a mechanism for estimating their frequency and intensity. In summer 2004, several strong tropical cyclones critically reduced LAI late in the mature period, thereby reducing GPP (Ito 2010). Although ongoing global warming may increase the intensity of extreme climatic events, both regionally and globally (Easterling et al. 2000; IPCC 2012), our current phenological model cannot predict or account for such events. Model GPP overestimated measured values by $77 \text{ g C m}^{-2} \text{ month}^{-1}$, compared with differences of -19 to $+25 \text{ g C m}^{-2} \text{ month}^{-1}$ for this period in years other than 2004 (Fig. 2). Ito (2010) successfully predicted defoliation intensity caused by each typhoon event at TKY via inverse estimation from the flux measurement data, using a Monte Carlo approach. One of our subsequent tasks will be to develop a predictive model of canopy phenology that accounts for the frequency and intensity of extreme events and calculates their impact on canopy phenology.

To further improve our phenology model, we should consider the canopy phenology of each tree species in the forest, including representation of the effects of interspecies longevity differences and of succession. Inoue et al. (2014) found differences in the start of leaf expansion and end of leaf-fall among tree species at TKY, and differences in their phenological sensitivity to

Table 4 Projected changes of production and respiration for whole ecosystem, overstory vegetation, and understory vegetation under global warming, during snow-cover period (December–March), leaf-expansion period (April–May), mature period (June–September), leaf-fall period (October–November), and total annual period

	Period	Production ($\text{g C m}^{-2} \text{ year}^{-1}$)			Respiration ($\text{g C m}^{-2} \text{ year}^{-1}$)		
		ΔGPP	ΔNPP	ΔNEP	ΔRE	ΔR_{au}	ΔR_{h}
Whole	Snow cover	6	0	−4	9	6	4
	Leaf expansion	58	41	34	24	17	7
	Mature	34	7	−18	51	27	24
	Leaf-fall	29	17	12	16	12	4
	Annual	126	65	26	101	62	39
Overstory	Snow cover	0	−4	−	7	4	−
	Leaf expansion	63	46	−	22	17	−
	Mature	37	12	−	44	25	−
	Leaf-fall	37	25	−	16	13	−
	Annual	137	78	−	89	59	−
Understory	Snow cover	6	4	−	2	1	−
	Leaf expansion	−5	−5	−	2	0	−
	Mature	−3	−5	−	7	2	−
	Leaf-fall	−9	−8	−	0	0	−
	Annual	−11	−14	−	12	3	−

Positive values indicate increase under projected future climate (2068–2073) compared with current climate (2002–2007). Italicized values represent periods that accounted for more than 40 % of annual value

GPP gross primary production, *NPP* net primary production, *NEP* net ecosystem production, *RE* ecosystem respiration, *R_{au}* autotrophic respiration; *R_h* heterotrophic respiration

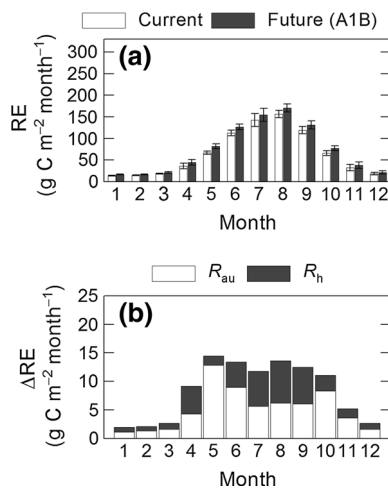


Fig. 6 Simulated seasonal variation of (a) ecosystem respiration (RE) under current (2002–2007) and future (2068–2073) climates, and (b) contributions of autotrophic (R_{au}) and heterotrophic (R_{h}) respiration to projected changes in total ecosystem respiration. Positive values in (b) indicate increase under projected future climate (2068–2073) relative to values under current climate (2002–2007). Range bars in (a) show standard deviation for data from the 6 years of each period

air temperature. Other recent studies have suggested that temperature sensitivity of canopy phenology differed among tree species (Noda et al. 2014; Polgar and Primack 2011, 2013) and warming experiments (Chung et al. 2013). This may mean that natural succession would change future temperature sensitivity of whole-ecosystem canopy phenology. In subsequent research, we should investigate the impact of canopy phenology on carbon budgets under ongoing global warming, by considering the natural succession that will occur and

differences in temperature sensitivity of canopy phenology among tree species. Long-term continuous field measurements of canopy phenology and warming experiments with respect to tree species would facilitate development of an improved canopy phenology model for each species.

Our comparison between the original and improved simulation results under current and future climate conditions demonstrates the importance of accounting for overstory canopy phenology, resulting effects on understory vegetation, and climate change impacts on this phenology. Although the advance in the date of overstory leaf expansion was similar to the delay in the date of overstory leaf-fall, our simulation results suggest that the earlier overstory leaf expansion had a greater effect on the increased production values. The main reason for this effect may be that earlier leaf expansion increased light interception by the overstory vegetation in late spring, during of the strongest solar radiation, thereby increasing carbon metabolic activity (carbon capture and release) of the overstory vegetation. In fact, cumulative absorbed PPFD (i.e., light interception) by that vegetation during the leaf-expansion period increased by $\sim 300 \text{ mol m}^{-2}$ under ongoing climate change, but only by $\sim 100 \text{ mol m}^{-2}$ during the leaf-fall period.

Our results also show the importance of light interception for the carbon budget of the understory vegetation. The contribution of understory GPP to whole-ecosystem GPP decreased slightly, from 11.3 % under the current climate to 9.1 % under the projected future climate. One of the main reasons for this change is the decline in total downward PPFD at the level of the understory vegetation during its photosynthetically ac-

tive period (by 11.8 % relative to the value under the current climate). Although that period lengthened, earlier overstory leaf expansion clearly increased light interception by the overstory vegetation and reduced that by the understory vegetation in spring, during of the strongest solar radiation. Several studies investigated living conditions of understory evergreen dwarf bamboo, revealing that coverage of the forest floor by that bamboo tended to decrease with increasing light interception by the forest canopy (Abe et al. 2005; Maki et al., 2008). If light interception by the understory vegetation decreases greatly as a result of earlier leaf expansion and later leaf-fall by the tree canopy in response to climate change, the bamboo habitat might shift to greater heights. Mapping and prediction of the cover of understory dwarf bamboo and an improved ecosystem model that predicts this effect will improve the accuracy of carbon budget predictions in eastern Asia. To achieve this goal, it will be necessary to accurately evaluate the spatiotemporal variability of understory evergreen dwarf bamboo and its environmental response via field observation, aircraft observation, and satellite remote sensing.

In future research, we recommend consideration of the spatial variation in canopy phenology and snow cover, since this would permit scaling-up of site-specific estimates of carbon budgets to local and regional scales. Several studies have suggested that the temperature sensitivity of canopy phenology (e.g., the start of leaf expansion and end of leaf-fall) varied along vertical (Vitasse et al. 2009a, b) and latitude (Hadano et al. 2013; Nagai et al. 2014) gradients, and that the nature of the variation depended on tree species or forest type. Therefore, if we use temperature sensitivity based on observations at a single site in predictions of future canopy phenology at regional scale, this could produce large errors in spatiotemporal patterns of canopy phenology and carbon budgets. To scale up the approach developed in the present study, it will be necessary to develop an empirical phenology model that considers latitudinal and vertical (altitude) gradients in canopy phenology. Prediction of annual variations in the start and end of the snow-cover period is another important issue for cool-temperate deciduous broadleaf forests with evergreen understory vegetation. For instance, central Japan has a wide range of altitude (500–3,000 m) over a relatively short distance (10–300 km). This vertical gradient creates strong regional differences in spatiotemporal patterns of the snow-cover period. To account for effects of these variations, accurate evaluation of the spatiotemporal variability of snow cover in a region will be required. Such information can be obtained by evaluating local meteorological parameters using a fine-scale meteorological model.

Consequently, our analysis clearly indicates the importance of understanding and accounting for the temporal variation and dynamics of canopy phenology and snow cover. Therefore, these factors should be incorporated in models used for the evaluation of carbon budgets in climate change studies. To improve understanding of these patterns and incorporate their

effects in studies of future carbon budgets using ecosystem models, researchers should promote interdisciplinary canopy phenology studies that link detailed and conventional ecosystem field observations (e.g., tree census data), in situ remote sensing using digital cameras and spectroradiometers, satellite remote sensing, and modeling. Future research should also include ecophysiological processes of canopy and understory vegetation to improve understanding of biological mechanisms that control canopy phenology.

Acknowledgments We thank S. Murayama of the National Institute of Advanced Industrial Science and Technology and N. Saigusa of the National Institute for Environmental Studies for providing detailed meteorological and eddy-covariance data for TKY. This work was supported by the Japan Society for the Promotion of Science (JSPS) KAKENHI program (Grant numbers 23710005 and 24241008) and by the JSPS Funding Program for Next Generation World-Leading Researchers (principal investigator H.M).

Appendix: photosynthetic and respiration components for the overstory vegetation

NCAR LSM is a sun and shade model. The sunlit fraction (f_{sun}) of the canopy is based on the fractional area of sunflecks on a horizontal plane below leaf and stem areas and on scattering within the canopy. The shaded fraction (f_{shade}) equals 1.0 minus the sunlit fraction, and the sunlit and shaded LAIs are [$L_{\text{sun}} = f_{\text{sun}}L$] and [$L_{\text{shade}} = f_{\text{shade}}L$], respectively, where L represents LAI. Bonan (1996) provides details of the calculation of incident solar radiation at canopy level and of the energy budget resulting from the radiation and water vapor balances. The photosynthetic part of LSM (Bonan 1996) is based on the parameterizations of Farquhar et al. (1980) and Collatz et al. (1991). Single-leaf photosynthesis of C_3 plants is controlled by the RuBP carboxylase-limited rate of carboxylation, maximum rate of carboxylation allowed by the capacity to regenerate RuBP, and the export-limited rate of carboxylation. The photosynthetic rate is coupled to the parameterization of stomatal resistance (Collatz et al. 1991) and is hence an integral part of the surface energy fluxes. These calculations are made for both the sunlit and shaded parts of the canopy (A_{sun} and A_{shade}) and are summed for the entire overstory canopy as [$\text{GPP}_o = A_{\text{sun}} \cdot L_{\text{sun}} + A_{\text{shade}} \cdot L_{\text{shade}}$].

Overstory deciduous plant respiration is separated into maintenance and growth respiration. Total maintenance respiration in the LSM is determined by the sum of foliar, stem, and root respiration as functions of leaf area index ($\text{m}^2 \text{m}^{-2}$) and temperature. Parameters are defined for foliar respiration at 25 °C ($\mu\text{mol CO}_2 \text{m}^{-2} \text{s}^{-1}$), stem biomass (kg m^{-2}), stem respiration at 25 °C ($\mu\text{mol CO}_2 \text{kg}^{-1} \text{s}^{-1}$), root biomass (kg m^{-2}), root respiration at 25 °C ($\mu\text{mol CO}_2 \text{kg}^{-1} \text{s}^{-1}$), and temperature sensitivity. Growth respiration is proportional to overstory net primary production (NPP_o).

References

- Abe S, Nashimoto M, Matsui R, Takeuchi T, Ishii T (2005) Prediction and mapping of cover degree of dwarf bamboo understory by using the GIS and classification tree. *Veg Sci* 22:103–111 (in Japanese with English abstract)
- Baldocchi D (2008) ‘Breathing’ of the terrestrial biosphere: lessons learned from a global network of carbon dioxide flux measurement systems. *Aust J Bot* 56:1–26. doi:10.1071/bt07151
- Bonan GB (1996) A land surface model (LSM version 1.0) for ecological, hydrological, and atmospheric studies: technical description and user’s guide. National Center for Atmospheric Research, Boulder, USA
- Botta A, Viovy N, Ciais P, Friedlingstein P, Monfray P (2000) A global prognostic scheme of leaf onset using satellite data. *Glob Chang Biol* 6:709–725. doi:10.1046/j.1365-2486.2000.00362.x
- Chen X, Xu L (2012) Phenological responses of *Ulmus pumila* (Siberian Elm) to climate change in the temperate zone of China. *Int J Biometeor* 56:695–706. doi:10.1007/s00484-011-0471-0
- Chung H, Muraoka H, Nakamura M, Han S, Muller O, Son Y (2013) Experimental warming studies on tree species and forest ecosystems: a literature review. *J Plant Res* 124:447–460. doi:10.1007/s10265-013-0565-3
- Churkina G, Schimel D, Braswell BH, Xiao X (2005) Spatial analysis of growing season length control over net ecosystem exchange. *Glob Chang Biol* 11:1777–1787. doi:10.1111/j.1365-2486.2005.01012.x
- Collatz GJ, Ball JT, Grivet C, Berry JA (1991) Physiological and environmental regulation of stomatal conductance, photosynthesis, and transpiration: a model that includes a laminar boundary layer. *Agric For Meteorol* 54:107–136. doi:10.1016/0168-1923(91)90002-8
- Easterling DR, Meehl GA, Parmesan C, Changnon SA, Karl TR, Mearns LO (2000) Climate extremes: observations, modeling, and impacts. *Sci* 289:2068–2074. doi:10.1126/science.289.5487.2068
- Farquhar GD, von Caemmerer S, Berry JA (1980) A biochemical model of photosynthetic CO₂ assimilation in leaves of C3 species. *Planta* 149:78–90
- Hadano M, Nasahara KN, Motohka T, Noda HM, Murakami K, Hosaka M (2013) High-resolution prediction of leaf onset date in Japan in the 21st century under the IPCC A1B scenario. *Ecol Evol* 3:1798–1807. doi:10.1002/ece3.575
- Inoue T, Nagai S, Saitoh TM, Muraoka H, Nasahara KN, Koizumi H (2014) Detection of the different characteristics of year-to-year variation in foliage phenology among deciduous broad-leaved tree species by using daily continuous canopy surface images. *Ecol Inf* 22:58–68. doi:10.1016/j.ecoinf.2014.05.009
- IPCC (2012) Managing the risks of extreme events and disasters to advance climate change adaptation. a special report of working groups I and II of the intergovernmental panel on climate change. Cambridge University Press, Cambridge, UK
- IPCC (2013) Climate change 2013: the physical science basis. Contribution of working group I to the fifth assessment report of the intergovernmental panel on climate change. Cambridge University Press, Cambridge and New York
- Ito A (2010) Evaluation of the impacts of defoliation by tropical cyclones on a Japanese forest’s carbon budget using flux data and a process-based model. *J Geophys Res* 115:G04013. doi:10.1029/2010jg001314
- Ito H, Hino T (2004) Effects of deer, mice and dwarf bamboo on the emergence, survival and growth of *Abies homolepis* (Piceaceae) seedlings. *Ecol Res* 19:217–223. doi:10.1111/j.1440-1703.2004.00626.x
- Jeong S-J, Medvigy D, Shevliakova E, Malyshev S (2012) Uncertainties in terrestrial carbon budgets related to spring phenology. *J Geophys Res* 117:G01030. doi:10.1029/2011jg001868
- Jia S, Akiyama T (2005) A precise, unified method for estimating carbon storage in cool-temperate deciduous forest ecosystems. *Agric For Meteorol* 134:70–80. doi:10.1016/j.agrformet.2005.08.014
- Maki M, Goto S, Ishihara M, Nishida K, Kojima T, Akiyama T (2008) Mapping the potential distribution of dwarf bamboo using satellite imagery and DEM. *J Remote Sens Soc Jpn* 28:28–35. doi:10.11440/rssj.28.28 (in Japanese with English abstract)
- Matsumoto K, Ohta T, Irasawa M, Nakamura T (2003) Climate change and extension of the *Ginkgo biloba* L. growing season in Japan. *Glob Chang Biol* 9:1634–1642. doi:10.1046/j.1529-8817.2003.00688.x
- Menzel A, Fabian P (1999) Growing season extended in Europe. *Nature* 397:659. doi:10.1038/17709
- Menzel A, Sparks TH, Estrella N, Koch E, Aasa A, Ahas R, Alm-Kübler K, Bissolli P, Braslavská OG, Briede A, Chmielewski FM, Crepinsek Z, Curnel Y, Dahl A, Defila C, Donnelly A, Filella Y, Jatczak K, Måge F, Mestre A, Nordli Ø, Peñuelas J, Pirinen P, Remišová V, Scheffinger H, Striz M, Susnik A, von Vliet AJH, Wielgolaski F-E, Zach S, Züst ANA (2006) European phenological response to climate change matches the warming pattern. *Glob Chang Biol* 12:1969–1976. doi:10.1111/j.1365-2486.2006.01193.x
- Michihiro Y, Sato Y, Suzuki Y (2011) Evaluation of reproducibility and uncertainty for surface meteorological elements over Japanese land area by the CMIP3 multi-climate models. *J Jpn Soc Hydrol Water Resour* 24:280–291. doi:10.3178/jjshwr.24.280 (in Japanese with English abstract)
- Morin X, Lechowicz MJ, Augspurger C, O’Keefe J, Viner D, Chuine I (2009) Leaf phenology in 22 North American tree species during the 21st century. *Glob Chang Biol* 15:961–975. doi:10.1111/j.1365-2486.2008.01735.x
- Muraoka H, Saigusa N, Nasahara KN, Noda H, Yoshino J, Saitoh TM, Nagai S, Murayama S, Koizumi H (2010) Effects of seasonal and interannual variations in leaf photosynthesis and canopy leaf area index on gross primary production of a cool-temperate deciduous broadleaf forest in Takayama, Japan. *J Plant Res* 123:563–576. doi:10.1007/s10265-009-0270-4
- Nagai S, Saitoh TM, Kurumado K, Tamagawa I, Kobayashi H, Inoue T, Suzuki R, Gamo M, Muraoka H, Nasahara KN (2013) Detection of bio-meteorological year-to-year variation by using digital canopy surface images of a deciduous broad-leaved forest. *SOLA* 9:106–110. doi:10.2151/sola.2013-024
- Nagai S, Saitoh TM, Nasahara KN, Suzuki R (2014) Spatio-temporal distribution of the timing of start and end of growing season along vertical and horizontal gradients in Japan. *Int J Biometeor*. doi:10.1007/s00484-014-0822-8
- Nasahara KN, Muraoka H, Nagai S, Mikami H (2008) Vertical integration of leaf area index in a Japanese deciduous broad-leaved forest. *Agric For Meteorol* 148:1136–1146. doi:10.1016/j.agrformet.2008.02.011
- Noda HM, Muraoka H, Nasahara KN, Saigusa N, Murayama S, Koizumi H (2014) Phenology of leaf morphological, photosynthetic, and nitrogen use characteristics of canopy trees in a cool-temperate deciduous broadleaf forest at Takayama, central Japan. *Ecol Res*. doi:10.1007/s11284-014-1222-6
- Ohtsuka T, Akiyama T, Hashimoto Y, Inatomi M, Sakai T, Jia S, Mo W, Tsuda S, Koizumi H (2005) Biometric based estimates of net primary production (NPP) in a cool-temperate deciduous forest stand beneath a flux tower. *Agric For Meteorol* 134:27–38. doi:10.1016/j.agrformet.2005.11.005
- Ohtsuka T, Mo W, Satomura T, Inatomi M, Koizumi H (2007) Biometric based carbon flux measurements and net ecosystem production (NEP) in a temperate deciduous broad-leaved forest beneath a flux tower. *Ecosyst* 10:324–334. doi:10.1007/s10021-007-9017-z
- Ohtsuka T, Saigusa N, Koizumi H (2009) On linking multiyear biometric measurements of tree growth with eddy covariance-based net ecosystem production. *Glob Chang Biol* 15:1015–1024. doi:10.1111/j.1365-2486.2008.01800.x
- Piao S, Friedlingstein P, Ciais P, Viovy N, Demarty J (2007) Growing season extension and its impact on terrestrial carbon cycle in the Northern Hemisphere over the past 2 decades. *Glob Biogeochem Cycles* 21:3018. doi:10.1029/2006gb002888

- Polgar CA, Primack RB (2011) Leaf-out phenology of temperate woody plants: from trees to ecosystems. *New Phytol* 191:926–941. doi:[10.1111/j.1469-8137.2011.03803.x](https://doi.org/10.1111/j.1469-8137.2011.03803.x)
- Polgar CA, Primack RB (2013) Leaf out phenology in temperate forests. *Biodivers Sci* 21:111–116. doi:[10.3724/SP.J.1003.2013.06187](https://doi.org/10.3724/SP.J.1003.2013.06187)
- Richardson AD, Bailey AS, Denny EG, Martin CW, O'Keefe J (2006) Phenology of a northern hardwood forest canopy. *Glob Chang Biol* 12:1174–1188. doi:[10.1111/j.1365-2486.2006.01164.x](https://doi.org/10.1111/j.1365-2486.2006.01164.x)
- Richardson AD, Hollinger DY, Dail DB, Lee JT, Munger JW, O'Keefe J (2009) Influence of spring phenology on seasonal and annual carbon balance in two contrasting New England forests. *Tree Physiol* 29:321–331. doi:[10.1093/treephys/tpn040](https://doi.org/10.1093/treephys/tpn040)
- Richardson AD, Anderson RS, Arain MA, Barr AG, Bohrer G, Chen G, Chen JM, Ciais P, Davis KJ, Desai AR, Dietze MC, Dragoni D, Garrity SR, Gough CM, Grant R, Hollinger DY, Margolis HA, McCaughey H, Migliavacca M, Monson RK, Munger JW, Poulter B, Raczka BM, Ricciuto DM, Sahoo AK, Schaefer K, Tian H, Vargas R, Verbeeck H, Xiao J, Xue Y (2012) Terrestrial biosphere models need better representation of vegetation phenology: results from the North American Carbon Program Site Synthesis. *Glob Chang Biol* 18:566–584. doi:[10.1111/j.1365-2486.2011.02562.x](https://doi.org/10.1111/j.1365-2486.2011.02562.x)
- Richardson AD, Keenan TF, Migliavacca M, Ryu Y, Sonnentag O, Toomey M (2013) Climate change, phenology, and phenological control of vegetation feedbacks to the climate system. *Agric For Meteorol* 169:156–173. doi:[10.1016/j.agrformet.2012.09.012](https://doi.org/10.1016/j.agrformet.2012.09.012)
- Saigusa N, Yamamoto S, Murayama S, Kondo H, Nishimura N (2002) Gross primary production and net ecosystem exchange of a cool-temperate deciduous forest estimated by the eddy covariance method. *Agric For Meteorol* 112:203–215. doi:[10.1016/S0168-1923\(02\)00082-5](https://doi.org/10.1016/S0168-1923(02)00082-5)
- Saitoh TM, Nagai S, Noda HM, Muraoka H, Nasahara KN (2012a) Examination of the extinction coefficient in the Beer-Lambert law for an accurate estimation of the forest canopy leaf area index. *For Sci Technol* 8:67–76. doi:[10.1080/21580103.2012.673744](https://doi.org/10.1080/21580103.2012.673744)
- Saitoh TM, Nagai S, Yoshino J, Muraoka H, Saigusa N, Tamagawa I (2012b) Functional consequences of differences in canopy phenology for the carbon budgets of two cool-temperate forest types: simulations using the NCAR/LSM and validation using tower flux and biometric data. *Eurasian J For Res* 15:19–30
- Sakai T, Akiyama T, Saigusa N, Yamamoto S, Yasuoka Y (2006) The contribution of gross primary production of understory dwarf bamboo, *Sasa senanensis*, in a cool-temperate deciduous broadleaved forest in central Japan. *For Ecol Manag* 236:259–267. doi:[10.1016/j.foreco.2006.09.022](https://doi.org/10.1016/j.foreco.2006.09.022)
- Schwartz MD, Ahas R, Aasa A (2006) Onset of spring starting earlier across the Northern Hemisphere. *Glob Chang Biol* 12:343–351. doi:[10.1111/j.1365-2486.2005.01097.x](https://doi.org/10.1111/j.1365-2486.2005.01097.x)
- Takagi K, Fukuzawa K, Liang N, Kayama M, Nomura M, Hojyo H, Sugata S, Shibata H, Fukazawa T, Takahashi Y, Nakaji T, Oguma H, Mano M, Akibayashi Y, Murayama T, Koike T, Sasa K, Fujinuma Y (2009) Change in CO₂ balance under a series of forestry activities in a cool-temperate mixed forest with dense undergrowth. *Glob Chang Biol* 15:1275–1288. doi:[10.1111/j.1365-2486.2008.01795.x](https://doi.org/10.1111/j.1365-2486.2008.01795.x)
- Tang CQ, Li T, Zhu X (2007) Structure and regeneration dynamics of three subtropical midmontane moist evergreen broad-leaved forests in southwestern China, with special reference to bamboo in the forest understories. *Can J For Res* 37:2701–2714. doi:[10.1139/X07-101](https://doi.org/10.1139/X07-101)
- Thornley JHM (1976) *Mathematical models in plant physiology*. Academic Press, London
- Vitasse Y, Delzon S, Dufrêne E, Pontailler J-Y, Louvet J-M, Kremer A, Michalet R (2009a) Leaf phenology sensitivity to temperature in European trees: Do within-species populations exhibit similar responses? *Agric For Meteorol* 149:735–744. doi:[10.1016/j.agrformet.2008.10.019](https://doi.org/10.1016/j.agrformet.2008.10.019)
- Vitasse Y, Porte AJ, Kremer A, Michalet R, Delzon S (2009b) Responses of canopy duration to temperature changes in four temperate tree species: relative contributions of spring and autumn leaf phenology. *Oecologia* 161:187–198. doi:[10.1007/s00442-009-1363-4](https://doi.org/10.1007/s00442-009-1363-4)
- Wu C, Chen JM, Black TA, Price DT, Kurz WA, Desai AR, Gonsamo A, Jassal RS, Gough CM, Bohrer G, Dragoni D, Herbst M, Gielen B, Berninger F, Vesala T, Mammarella I, Pilegaard K, Blanken PD (2013a) Interannual variability of net ecosystem productivity in forests is explained by carbon flux phenology in autumn. *Glob Ecol Biogeogr* 22:994–1006. doi:[10.1111/geb.12044](https://doi.org/10.1111/geb.12044)
- Wu C, Gough CM, Chen JM, Gonsamo A (2013b) Evidence of autumn phenology control on annual net ecosystem productivity in two temperate deciduous forests. *Ecol Eng* 60:88–95. doi:[10.1016/j.ecoleng.2013.07.019](https://doi.org/10.1016/j.ecoleng.2013.07.019)
- Yashiro Y, Shizu Y, Adachi T, Ohtsuka T, Lee N-Y, Iimura Y, Koizumi H (2012) The effect of dense understory dwarf bamboo (*Sasa senanensis*) on soil respiration before and after clearcutting of cool temperate deciduous broad-leaved forest. *Ecol Res* 27:577–586. doi:[10.1007/s11284-012-0925-9](https://doi.org/10.1007/s11284-012-0925-9)